Electronic Supplementary Material (ESI) for RSC Advances.

Supporting information

Surface-Enhanced Raman Scattering-Active Desert-Rose-Like Ag Mesoparticles Prepared Using Cyclic Voltammetric Methods

You-Hong You, Yang-Wei Lin, and Chung-Yu Chen*

Department of Chemistry, National Changhua University of Education, Changhua, Taiwan

Address correspondence to these authors at Department of Chemistry, National Changhua University of Education, Changhua City, PO Box 500, Taiwan; Fax:; E-mail: linywjerry@cc.ncue.edu.tw

Table S1. SERS EFs of the different substrates

Name	Constituents	I_{bulk}[a]	N_{bulk}	I_{SERS}	N_{SERS}	B[b]	EF[c]	Remarks
4-MBA/SPCE	4-MBA powder spread on SPCE	1246	2.0×10^{12}	-	-	-	-	Inherent Raman of 4-MBA
Ag/SPCE	Irregularly shaped Ag particles deposited on SPCE	-	-	874	7.2×10^{7}	0.8	2.5×10^{4}	See text for synthesis and characteristics
DR_Ag/SPCE	Desert-rose-like Ag mesoparticles deposited on SPCE	-	-	29960	7.5×10^{8}	0.5	1.3×10^{5}	See text for synthesis and characteristics

[a]Raman intensity is the intensity of the Raman peak at 1582 cm^{-1}

[b]B (hindrance) is defined in eq. (2) in the text

[c]EF is defined in eq. (1) in the text

Table S2. Reproducibility test for desert-rose-like Ag mesoparticles deposited on the SPCE

Raman intensity	Intra-day		Inter-day	
Substrate	1075 cm^{-1} (±RSD%)[a]	1582 cm^{-1} (±RSD%)	1075 cm^{-1} (±RSD%)	1582 cm^{-1} (±RSD%)
1	720.1 (±4.1%)	1227.0 (±1.9%)	719.7 (±5.1%)	1229.7 (±6.7%)
2	718.3 (±3.2%)	1223.2 (±1.9%)	711.1 (±2.2%)	1225.5 (±1.9%)
3	711.1 (±2.2%)	1225.5 (±1.9%)	709.5 (±2.1%)	1230.3 (±4.3%)

[a]RSD (relative standard derivation) is calculated by dividing the standard deviation by the mean value of the data set (n = 3).

Table S3. The preparation processes, EFs, durability, and applications of various desert-rose-like metal structures deposited on SERS substrates

Substrate	Preparation process	EFs	Durability	Applications	Ref.
Au nanoflakes on quartz	Supramolecular templates and sputtering process (two-step method)	2.4×10^4 for 4-ATP	[a]	[a]	1
Flower-like Au nanostructure array on Si	Photolithography and electrodeposition (two-step method)	[a]	[a]	Adenine/DNA	2
Ag nanodesert rose on Si	Galvanic displacement process (one-step method)	3.0×10^4 for NPE 2.0×10^5 for 4-MPy 2.0×10^{10} for R6G	[a]	[a]	3
Au nanoflake on Si	Peptide mesocrystal templates and sputtering process (two-step method)	2.0×10^4 for 4-MBA	[a]	[a]	4
Flower-like Ag microstructures on a glass plane	Chemical reduction on PANI/PVA composite film (two-step method)	1.9×10^5 for 4-MBA	[a]	[a]	5
Ag mesoparticles on a SPCE	One step electrochemical reduction	1.3×10^5 for 4-MBA	150 °C/30 days	FAH gene	This study

[a]not provided

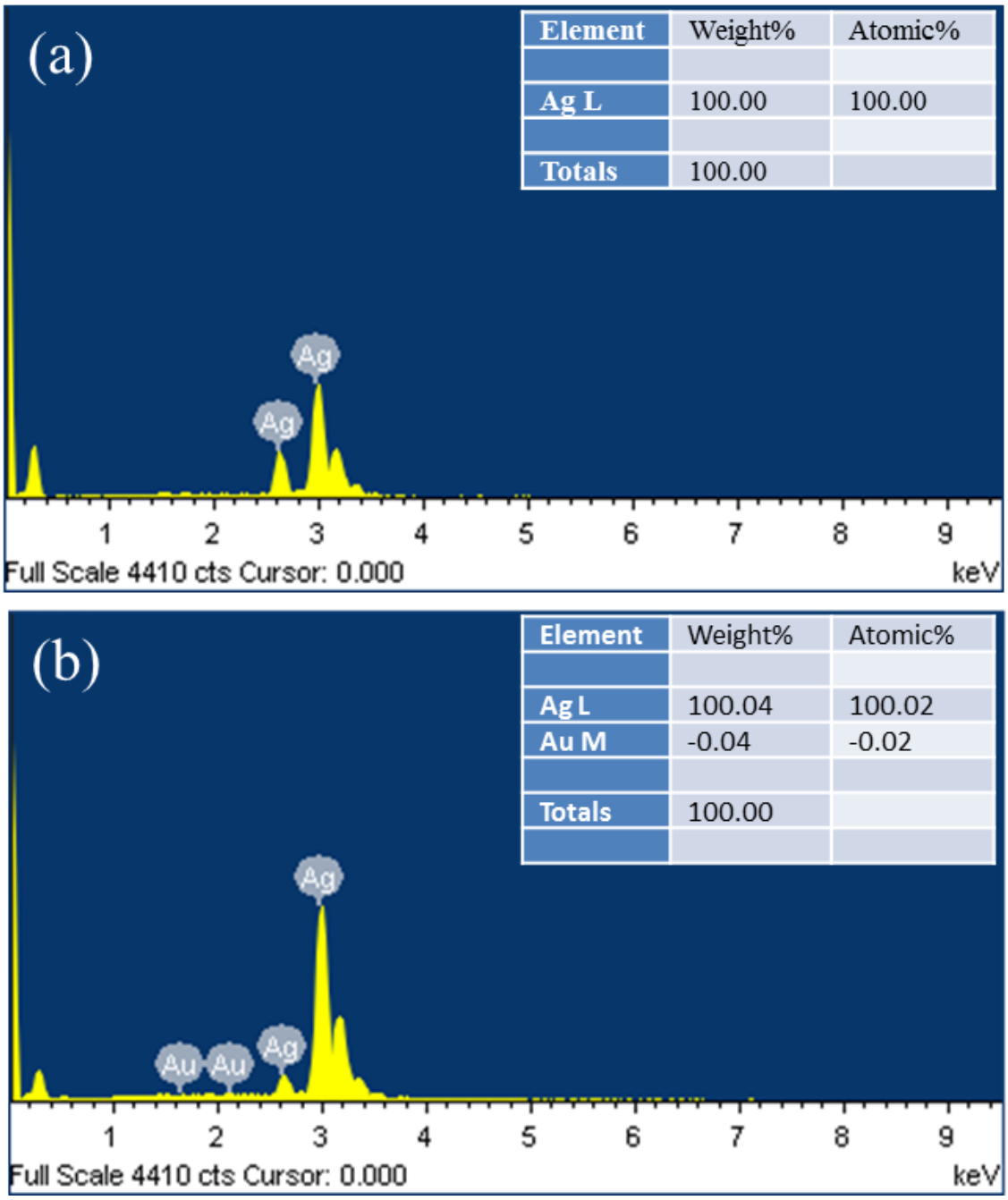

Figure S1. energy-dispersive X-ray spectroscopy (EDS) spectra of the (a) irregularly shaped Ag particles and (b) desert-rose-like Ag mesoparticles on SPCE.

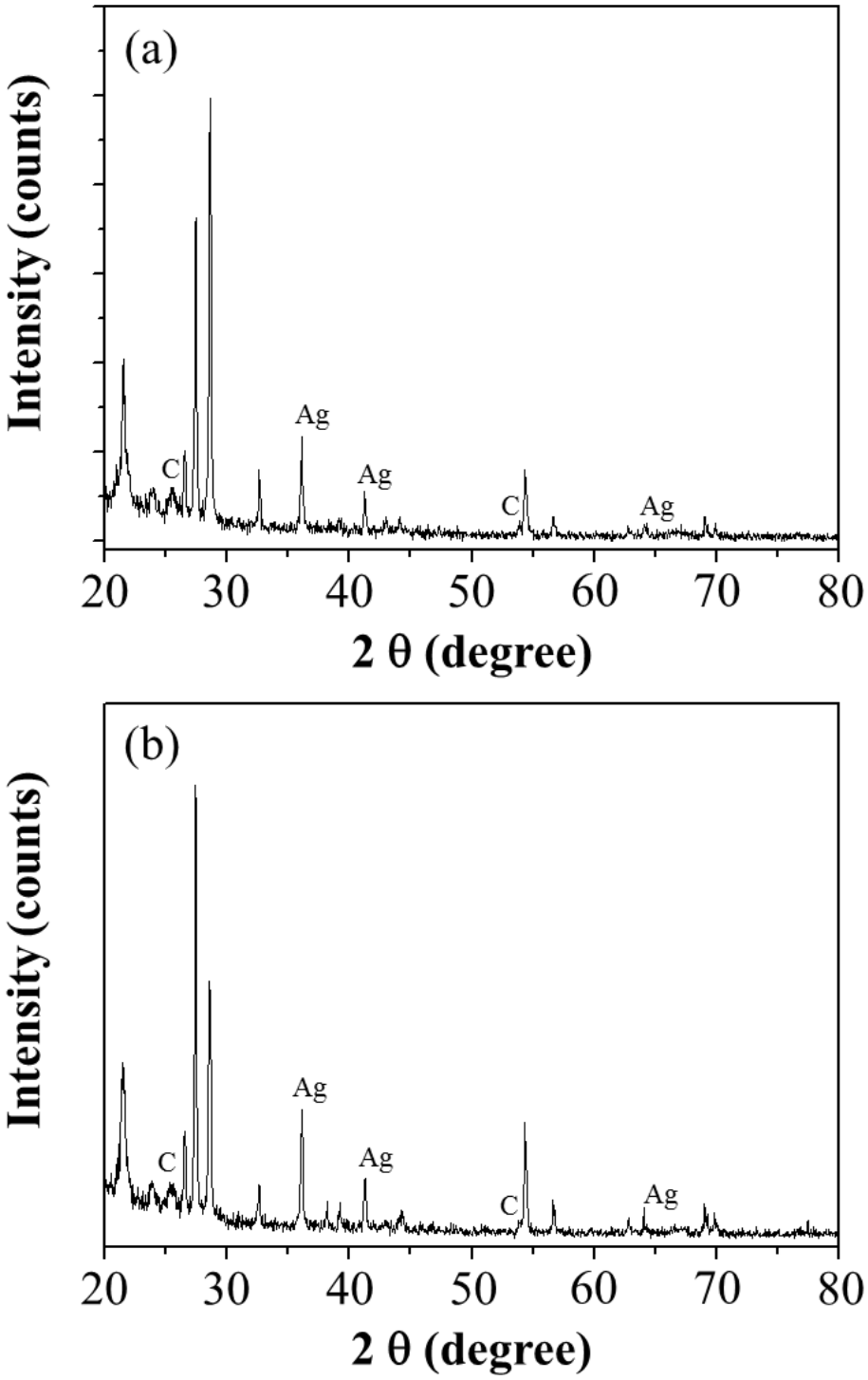

Figure S2. High resolution X-ray powder diffraction (HRXRD) spectra of the (a) irregularly shaped Ag particles and (b) desert-rose-like Ag mesoparticles on SPCE.

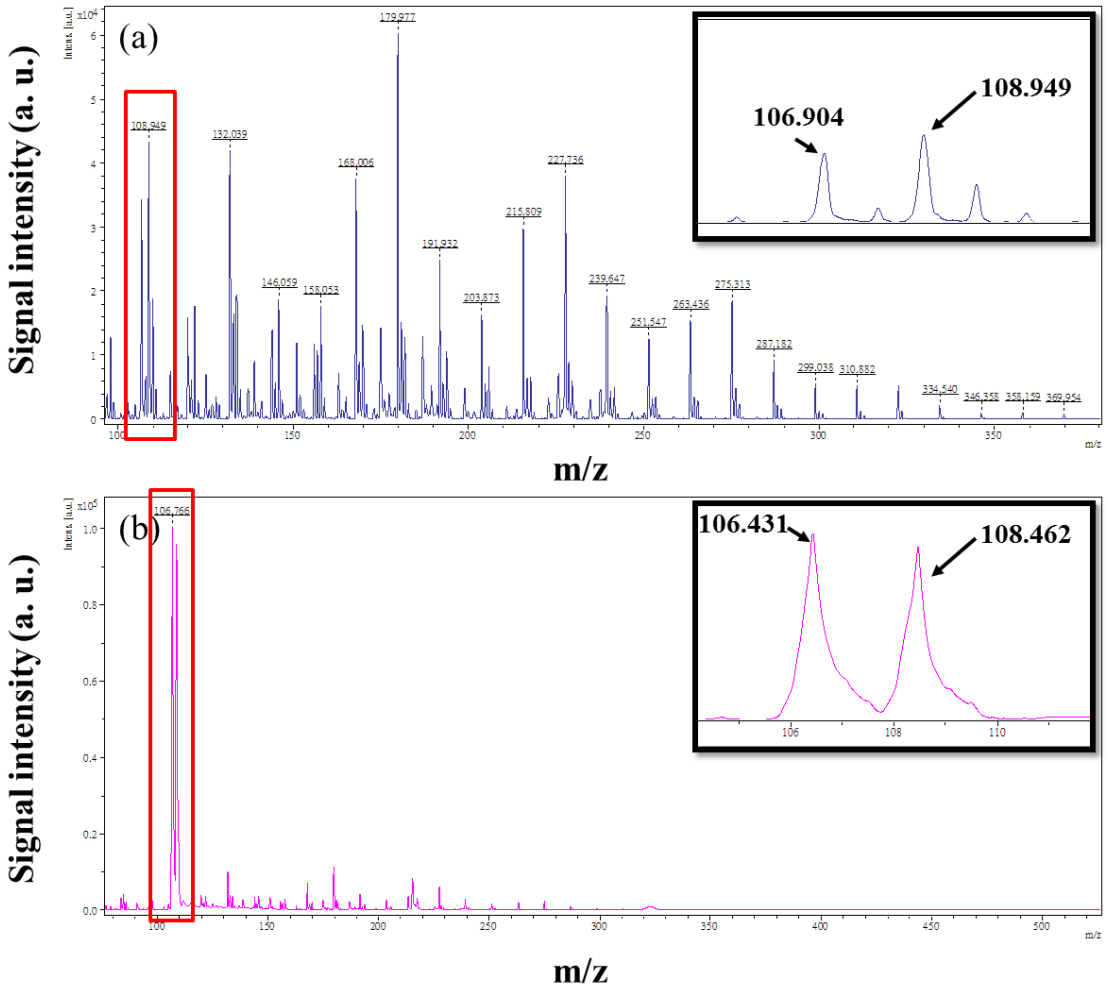

Figure S3. Surface-assisted laser desorption/ionization mass spectrometry (SALDI-MS) spectra of the (a) irregularly shaped Ag particles and (b) desert-rose-like Ag mesoparticles on SPCE.

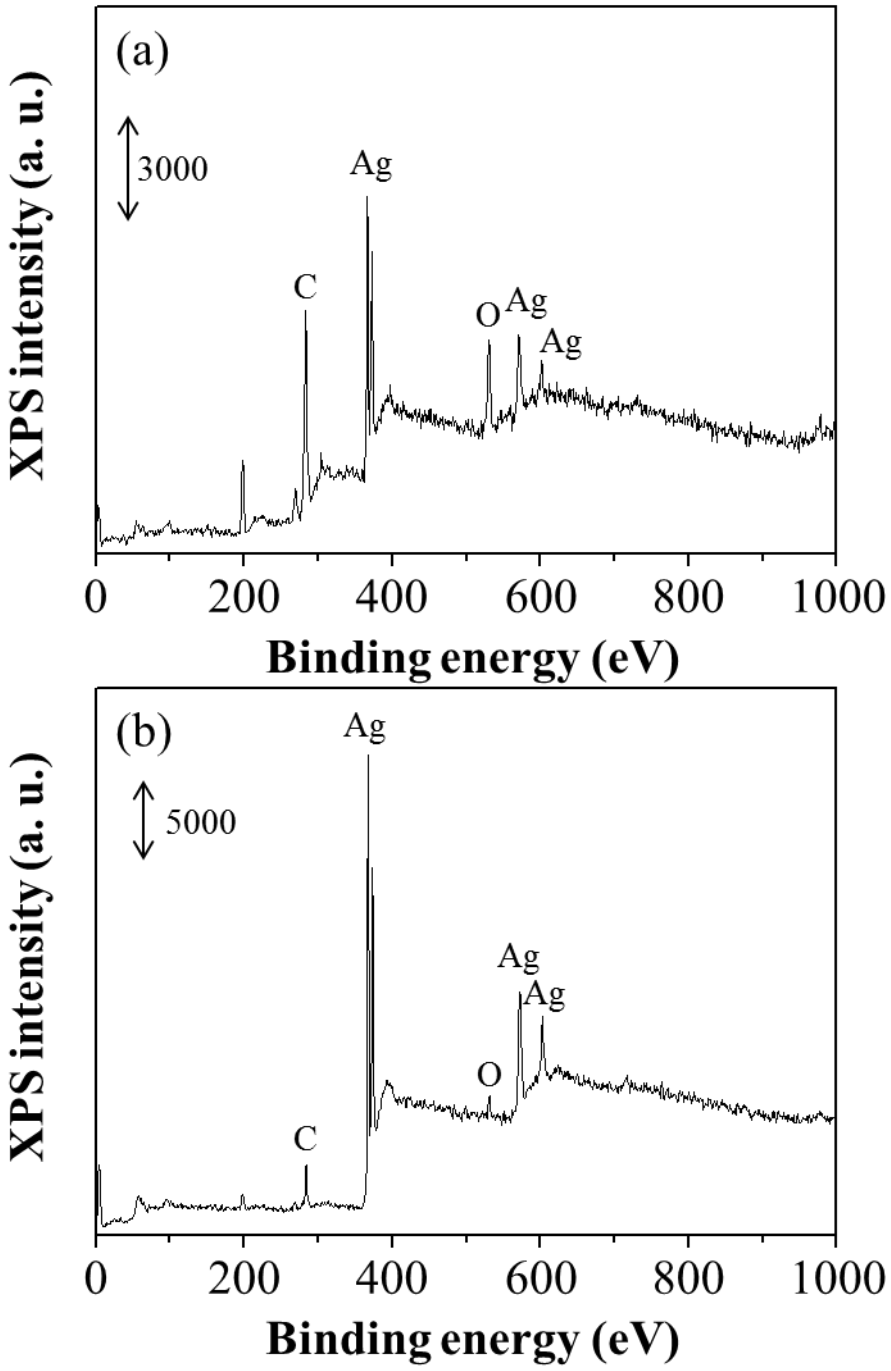

Figure S4. X-ray photoelectron spectroscopy (XPS) spectra of the (a) irregularly shaped Ag particles and (b) desert-rose-like Ag mesoparticles on SPCE.

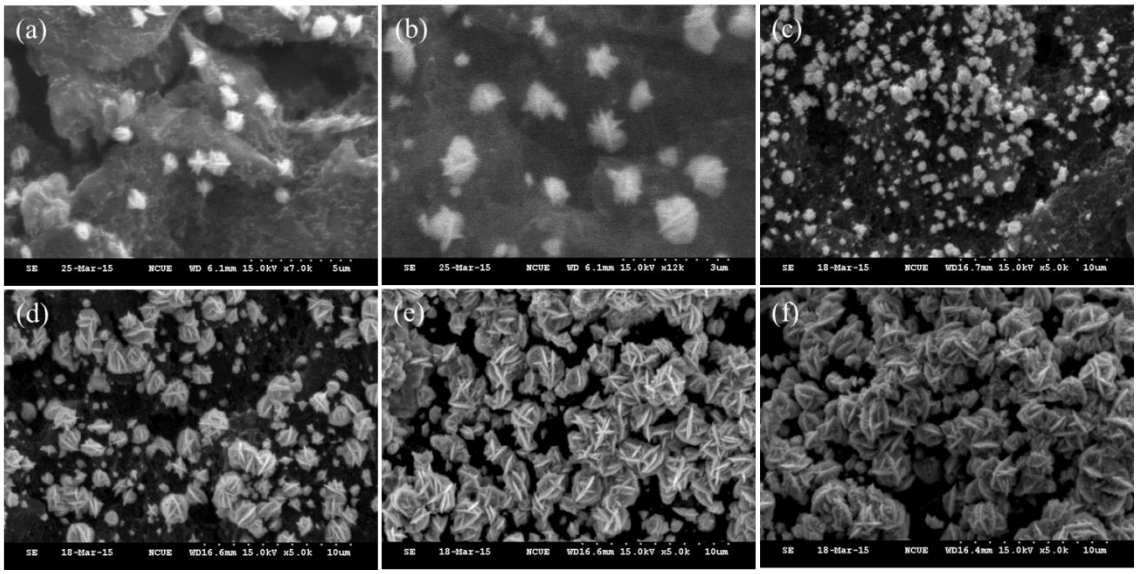

Figure S5. Representative SEM images of the desert-rose-like Ag mesoparticles at various electrodeposition times: (a) 1 min; scale bar = 5 mm, (b) 3 min; scale bar = 3 mm, (c) 5 min, (d) 15 min, (e) 30 min, and (f) 45 min. Scale bar = 10 mm in (c)–(f).

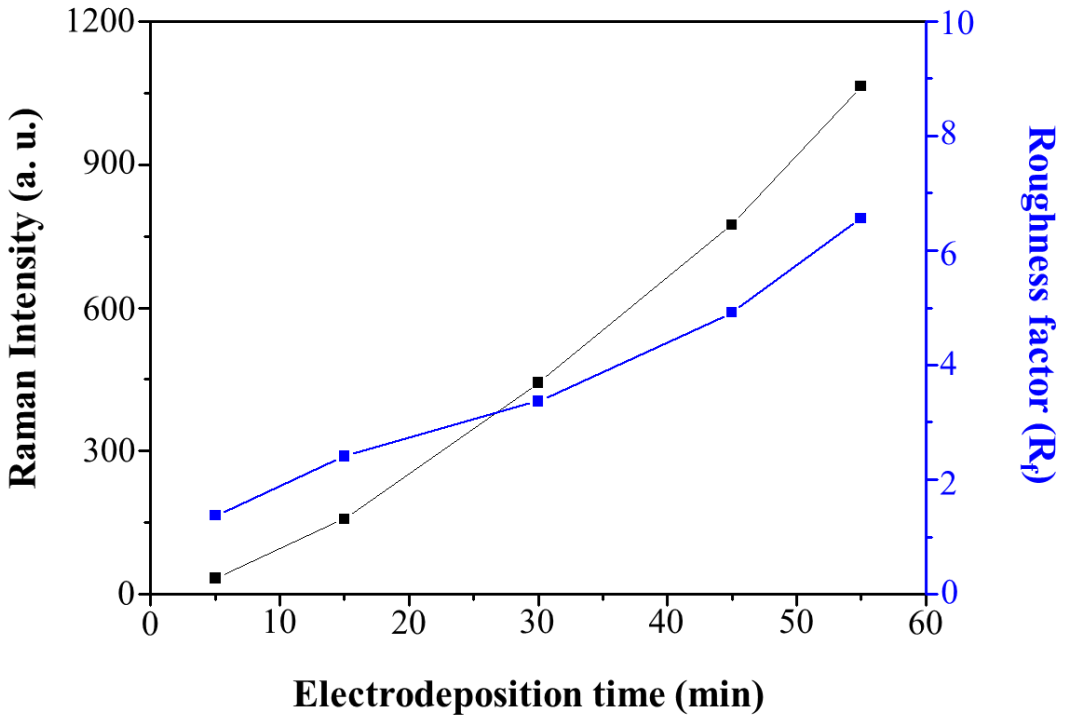

Figure S6. The relationship among the electrodeposition time, roughness factor, and Raman intensity of the desert-rose-like Ag mesoparticles.

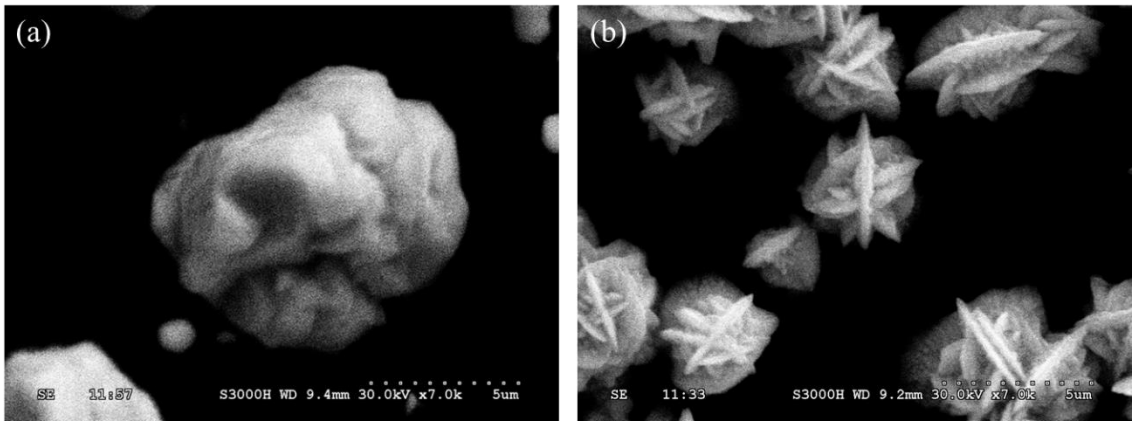

Figure S7. SEM images of Ag structures prepared in 10 mM $AgNO_3$ aqueous solution containing the (a) precipitates and (b) supernatants of 0.36 nM Au NP (diameter: 13.3 ± 1.7 nm) suspensions.

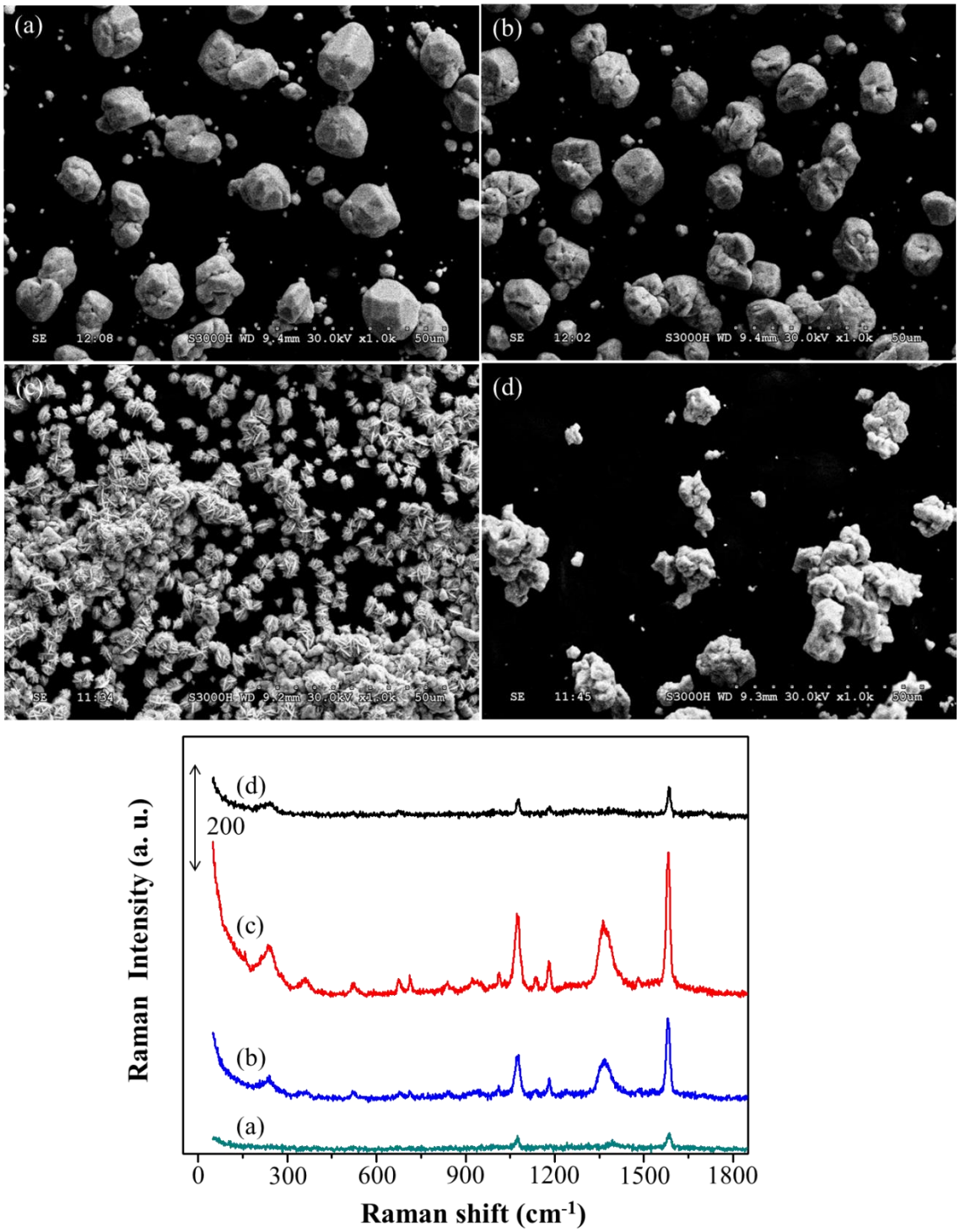

Figure S8. SEM images and SERS spectra of 4-MBA (10^{-5} M) molecules adsorbed onto Ag substrates fabricated by 10 mM Ag^{+} deposition solution containing various concentrations of sodium citrate: (a) 10^{-7}, (b) 10^{-6}, (c) 10^{-5}, and (d) 10^{-4} M.

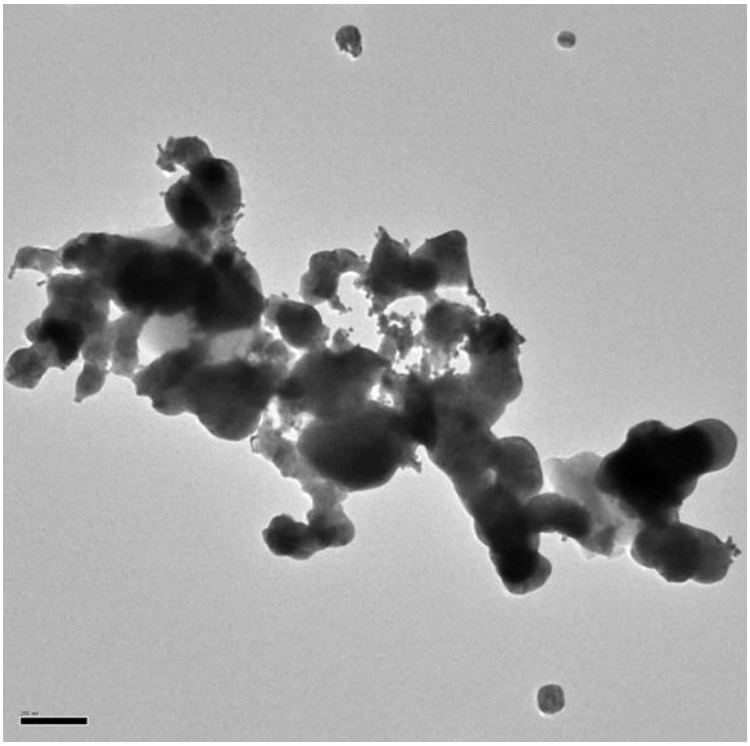

Figure S9. TEM images of 10 mM Ag^{+} depsotion solutions containg Au NP suspensions (0.36 nM; diameter: 13 nm).

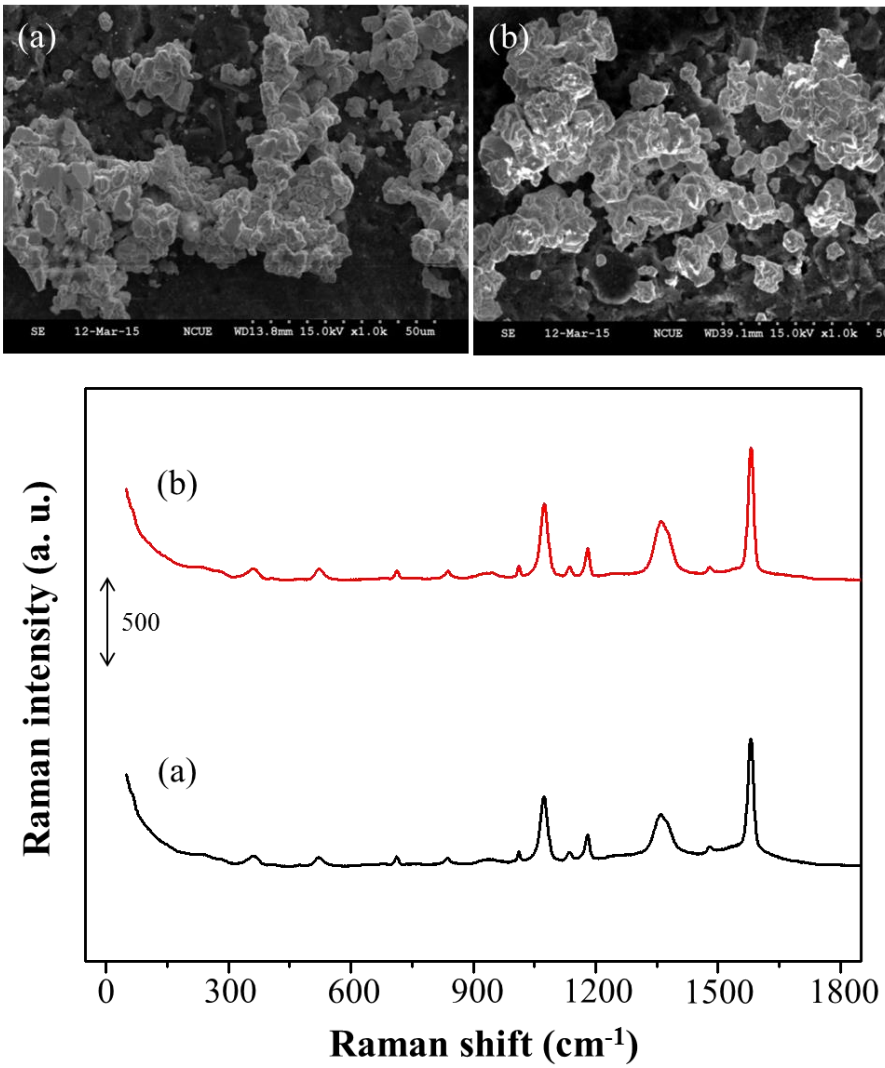

Figure S10. SEM images and SERS spectra of 4-MBA (10^{-5} M) molecules adsorbed onto Ag substrates in various deposition solutions: (a) 10 mM Ag^{+} ions and 32 nm Au NPs, and (b) 10 mM Ag^{+} ions and 56 nm Au NPs.

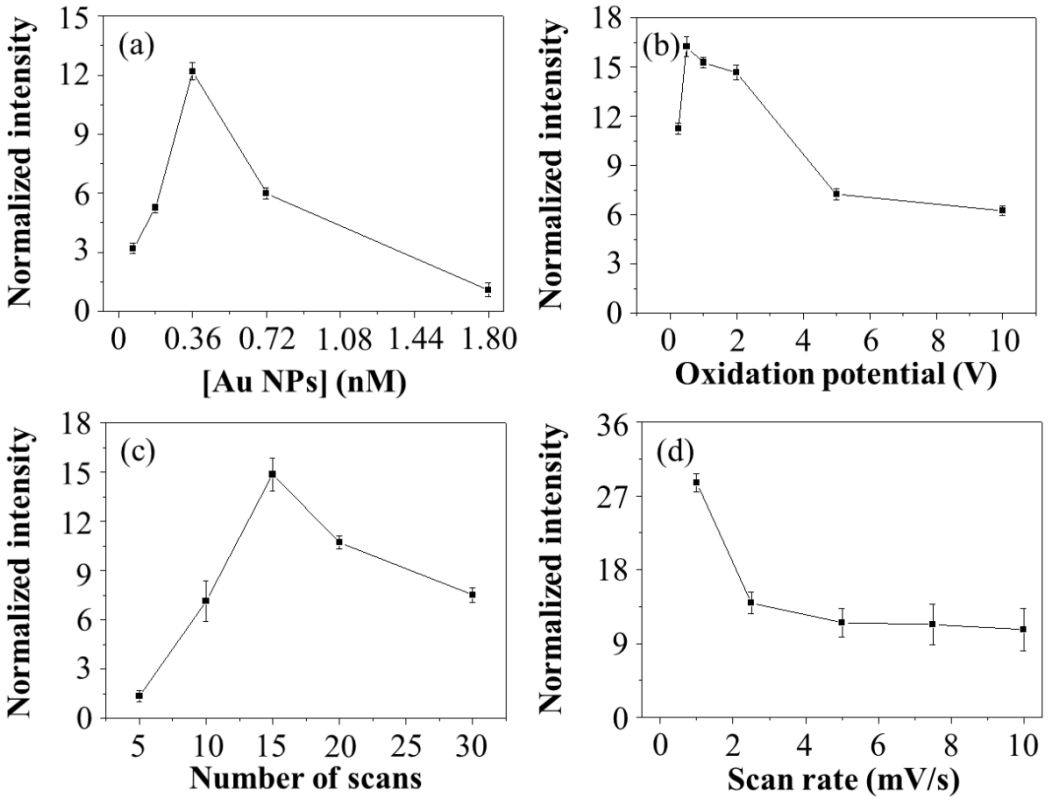

Figure S11. Normalized Raman intensity of 10^{-5} M 4-MBA adsorbed onto the Ag structures at different (a) concentrations of 13 nm Au NPs, (b) oxidation potentials, (c) number of deposition scans, and (d) deposition scan rates.

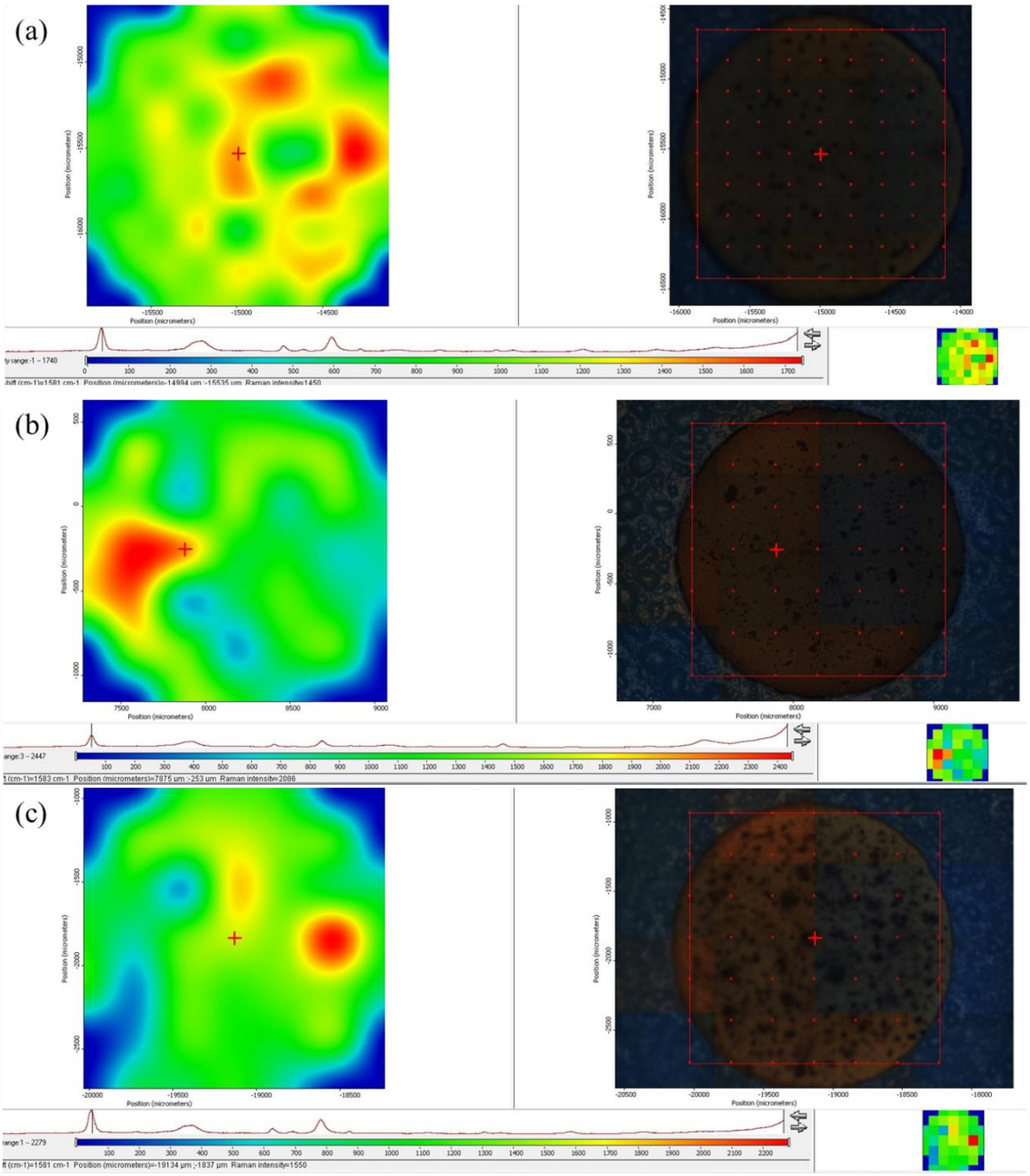

Figure S12. Raman mapping images of 4-MBA on three batches of desert-rose-like Ag substrates.

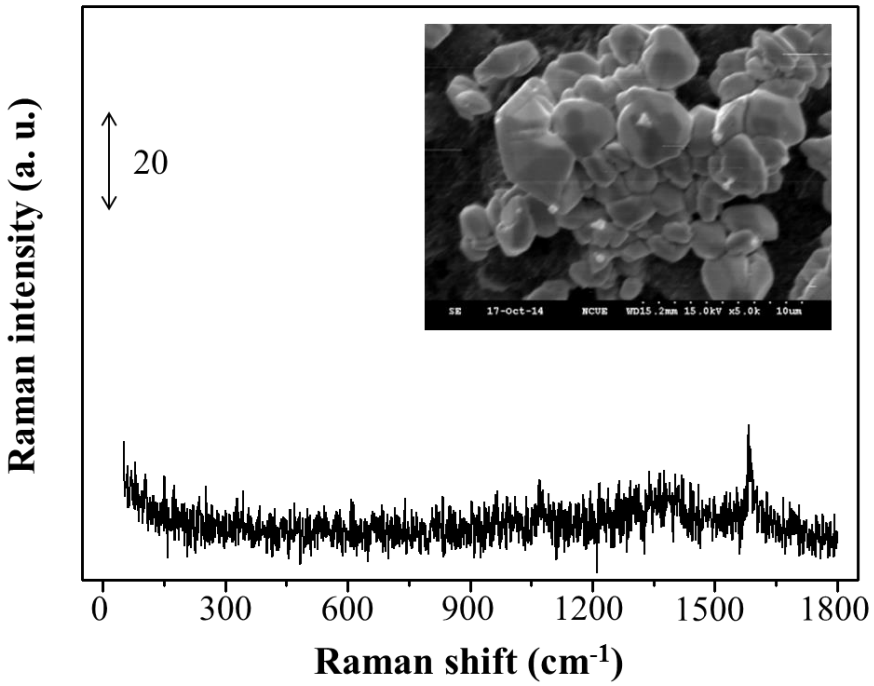

Figure S13. Raman spectra of 4-MBA adsorbed onto irregularly shaped Ag particles at 80 °C. Inset: SEM images of Ag particles on SPCE at 80 °C.

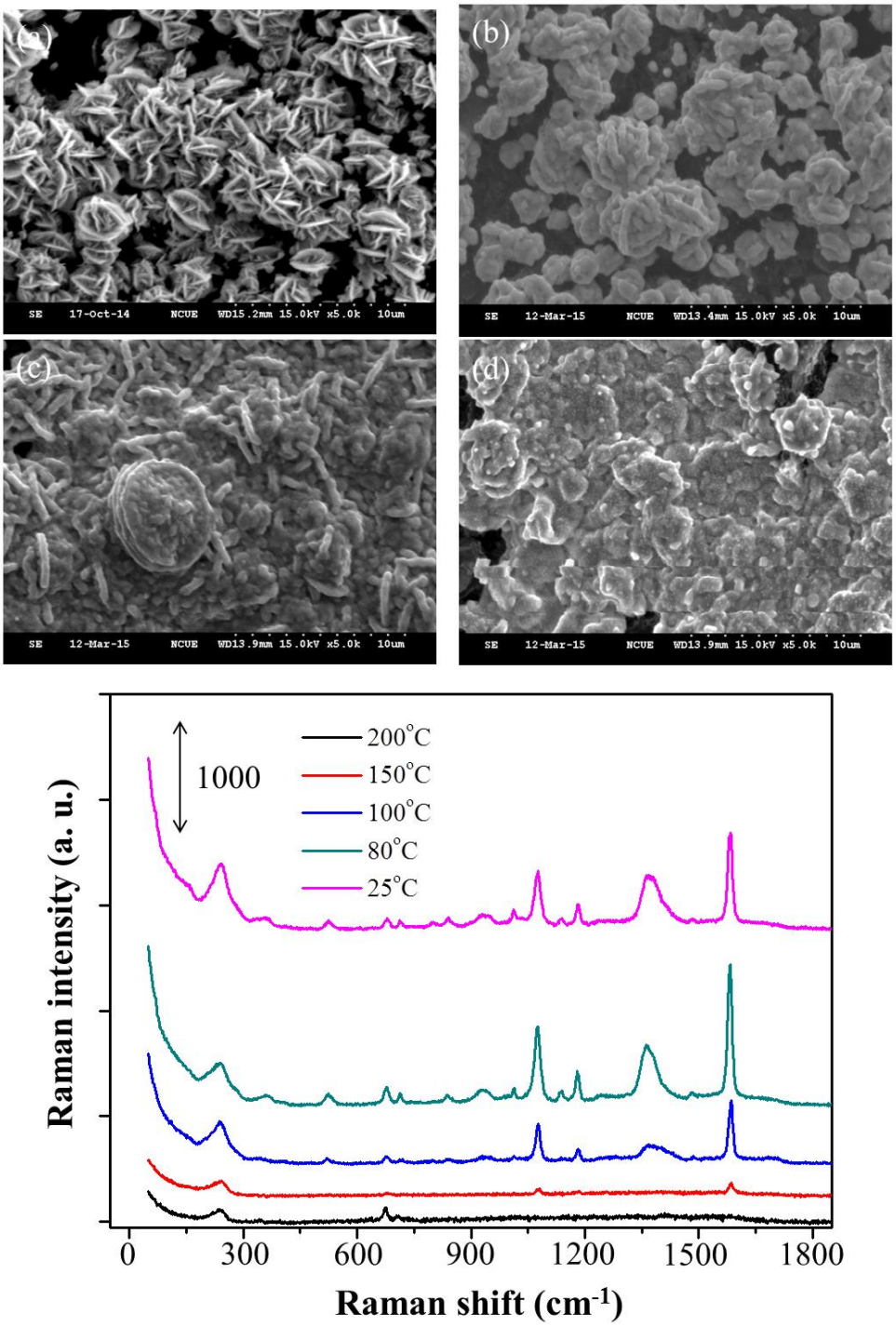

Figure S14. SEM images and Raman spectra of 4-MBA on Ag structures at various temperatures:(a)80 °C, (b) 100 °C, (c) 150 °C, and (d) 200 °C.

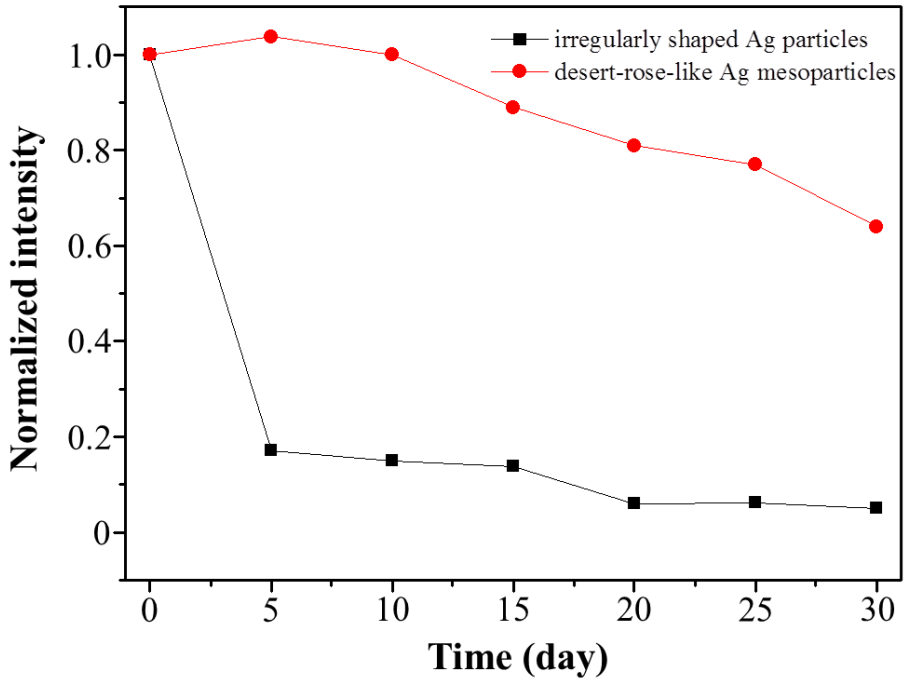

Figure S15. Variation in the normalized Raman intensity of 4-MBA adsorbed onto the irregularly shaped Ag particles (black) and desert-rose-like Ag mesoparticles (red) in 50% RH and 20% O_2 at 25 °C for 30 days.

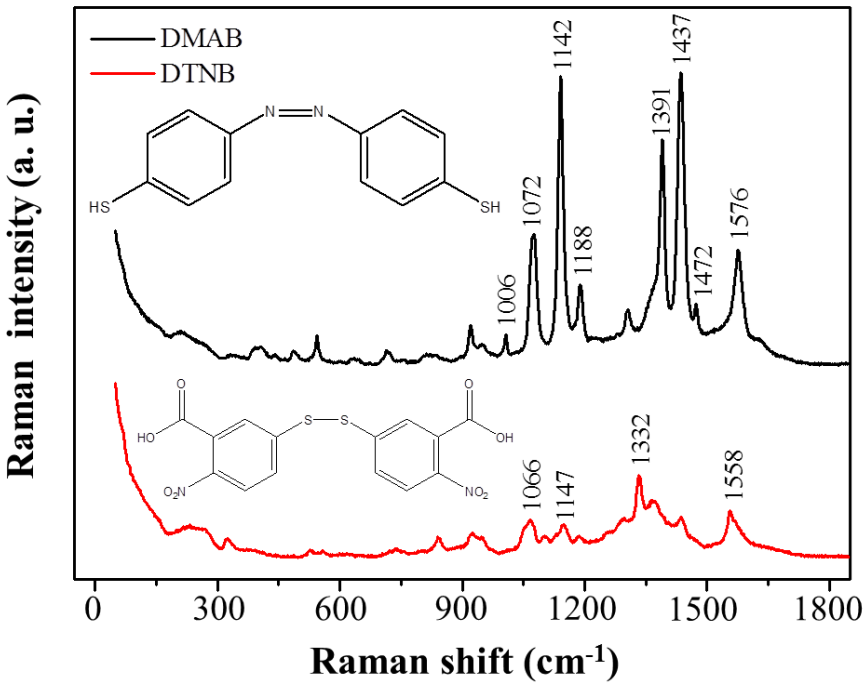

Figure S16. Raman spectrum of 10^{-5} M DMAB and DTNB molecules adsorbed onto the desert-rose-like Ag mesoparticles.

References

1. Y. F. Shen, J. B. Wang, U. Kuhlmann, P. Hildebrandt, K. Ariga, H. Mohwald, D. G. Kurth and T. Nakanishi, *Chem-Eur. J.*, 2009, **15**, 2763-2767.
2. J. H. Kim, T. Kang, S. M. Yoo, S. Y. Lee, B. Kim and Y. K. Choi, *Nanotechnology*, 2009, **20**.
3. A. Gutes, C. Carraro and R. Maboudian, *ACS App. Mater. Inter.*, 2009, **1**, 2551-2555.
4. Y. Su, Q. He, X. H. Yan, J. B. Fei, Y. E. Cui and J. B. Li, *Chem-Eur. J.*, 2011, **17**, 3370-3375.
5. Y. Y. Xia, T. J. Li, C. Gao, C. Ma and J. Chen, *J. Mater. Sci.*, 2014, **49**, 2781-2786.